FRACTURE PROPERTIES OF CONCRETE UNDER CRYOGENIC CONDITIONS

C. Rocco[1], J. Planas[2], G.V. Guinea[2] and M. Elices[2].

[1] Departamento de Construcciones, Facultad de Ingeniería, Universidad Nacional de La Plata
calle 48 y 115, La Plata, CP1900, Argentina
[2] Department of Materials Science, Escuela de Ingenieros de Caminos
Universidad Politécnica de Madrid, 28040 Madrid, Spain

ABSTRACT

In this paper, the fracture properties of a conventional concrete, at temperatures ranging from 20 to –170°C are reported. Two sets of test were carried out: a) stable three point bend tests on notched beams, conducted in CMOD control, and b) standard cylinder-splitting test. The tests were performed at 20, –20, –70, –120 and –170°C. To cool the specimens, two cryogenic chambers with automatic temperature control were used. From these tests, typical fracture parameters were determined according to cohesive crack model: tensile strength, fracture energy, softening curve, characteristic length and modulus of elasticity. The results show that low temperatures improve the fracture properties of concrete. As the temperature decreases, the tensile strength and the fracture energy increase markedly, especially until –70°C. Below this temperature, these properties tend to increase slowly or remain constant. From 20 to –170°C, concrete shows a two-fold increase in tensile strength and a three-fold increase in fracture energy. With regard to the softening curves, the results show that a bilinear approximation is a good estimate even for temperatures as low as –170 °C, and the shape of the curve is very similar at –120°C or higher temperatures. A significant difference in the shape, with a much shorter tail, is found at –170°C. The evolution of the characteristic length with temperature shows that the intrinsic brittleness of concrete decreases strongly as the temperature is reduced to –120°C, with a change in this trend when the concrete is cooled to –170°C.

INTRODUCTION

Concrete structures at low temperatures are currently used for the storage of liquefied gases, barge hulls, floating terminals and drilling hulls. In these applications, temperatures as low as –170ºC can be expected in service. It is known that standard concrete properties such as compressive strength, tensile strength, rupture modulus and modulus of elasticity can increase markedly at low temperatures. The tests results reported by differents authors [1, 2, 3] show that, depending on the water content, the concrete compressive strength at low temperatures can increase up to 400% over that at 20ºC. The dependence of the tensile strength on temperature, as determined by splitting, bending or double punch tests, is similar to the compressive strength, though less pronounced. The stress-strain response of axially compressed concrete is also influenced by the temperature and moisture content. As the temperature decreases, the nonlinearity of the stress-strain curve of concrete decreases.

Although the effect of the low temperature on the standard concrete properties, as mentioned above, has long been studied and the results show that at low temperatures the concrete exhibits many desirable features for the design engineer, less is known about the fracture properties of concrete in cryogenic conditions. One question has not been yet answered: is the concrete behaviour more brittle at low temperatures? Even though from fracture tests conducted by the authors [4, 5], it was shown that in saturated concrete the fracture energy is above that at room temperature, more information is needed to answer this question. In particular, there are no reports on the cohesive crack behaviour at low temperatures.

In this paper, the fracture properties of a conventional concrete, at temperatures ranging from 20 to –170°C are reported. Two sets of tests were carried out: a) stable three-point-bend tests on notched beams, conducted in CMOD control, and b) a standard cylinder-splitting tests. The elastic modulus and the bilinear approximation of the curve of stress vs. crack opening (softening curve) were determined at each test temperature. The evolution of typical fracture with temperature parameters associated with the cohesive crack (tensile strength, fracture energy, characteristic length) is also given.

MATERIALS AND SPECIMENS

To evaluate the fracture properties of concrete in cryogenic conditions, a typical concrete as used for building land-based storage of liquefied gases was used. To make the concrete, a crushed limestone of angular particles of a nominal maximum size of 20 mm, natural siliceous sand and ordinary portland cement similar to ASTM type I were used, with three different chemical additives: a sodium naphthalene sulfonate type superplasticizer, a non retarder plasticizer, and an air admixture. In mixing cement, sand and coarse aggregate were dry blended, and water was added with the additives. Details of the concrete mix proportions are given in Table 1.

TABLE 1

MIX PROPORTIONS OF CONCRETE

Cement kg/m^3	Water kg/m^3	Limestone kg/m^3	Sand kg/m^3	SF kg/m^3	P kg/m^3	AE kg/m^3
400	180	1056	912	2.8	4.8	0.28

SF superplasticizer, P plasticizer, AE air incorporating admixture.

Two sets of specimens were prepared and tested: a) cylindrical specimens of 150 mm length and 75 mm diameter for the splitting tensile test, and b) prismatic specimens of 100 x 100 x 470 mm for stable three point bend tests. All the specimens were cast from a single batch in steel moulds, compacted on a vibrating table, and inmediately stored in a controlled curing chamber at 20ºC and 95% r.h. during 24 hours. Next the specimens were demolded, immediately wrapped in a plastic polyethilene film and coated with paraffin wax to avoid moisture losses and microcracking. In these conditions, the specimens were stored in laboratory environment conditions until the time of the test 60 days later. Just before the three-point-bend test, 50 mm length notches were cut into the specimen thickness on the middle section of the prismatic specimens using a diamond saw. The width of the notches was 2 mm.

To measure the specimen temperature during the test, four type K thermocouples were attached to each specimen, two inside the specimen and two on the specimen surface. The inside thermocouples were embedded into the specimen during casting while those on the surface were fixed immediately before the test.

EXPERIMENTAL PROCEDURE

To determine the fracture properties of concrete, splitting tensile test and stable three point bend tests were performed according to ASTM C496, and the RILEM TC50 standard recommendations respectively [6,7].

The special features of the procedures are presented below:

Low temperature equipment
To cool the specimens to the test temperature, two low temperature chambers differing only in volume, were used throughout the experimentation. The temperature inside the chamber is lowered at a constant rate by spraying a mist of liquid nitrogen controlled by an electromagnetic valve. The intended cooling ramp is input to the temperature controller via a digital funtion generator, and the feed-back signal is provided by a platinum resistor sensing the gas coolant temperature. The controller automatically operates the electrovalve through a PID control algorithm. The stability of the gas temperature achieved with this system is ± 1.5ºC. During cooling, the gas coolant temperature and the temperature of the four type K thermocouples attached to the specimens are continuously recorded via an Automatic Data Acquisition System. The temperature stability at the specimen points is better than 0.1ºC.

The cooling rates used were 64ºC/hour for splitting test specimens and 32ºC/hour for three-point-bend test specimens. These cooling rates were selected to minimize the thermally induced stress in the specimen bulk, to avoid microcracking and noticeable damage at the notch root.

Splitting tensile test
Tests were performed at 20, –20, –70, –120 and –170°C, using a 1000 kN servohydraulic universal testing machine Instron 1275 with 8500 digital electronic control. At each temperature, three specimens were tested.

The tests were carried out under displacement control following the ASTM C496 standard recommendation at a displacement rate of 0.15 mm/minute. This rate was selected so that the tensile stress rate in the specimen remained below 1 MPa/minute throughout the test.

Once the test temperature was reached in the specimen, the load was applied continuously until the rupture of the specimen. The bearing strips used to distribute the load on the specimen were of plywood, free of imperfections, 3 mm thick and of 5 mm width. These bearing strips were glued to the specimen in the correct position before the test and were not reused. During the test the load and the temperatures of the thermocouples attached to the specimen were continuously recorded via an Automatic Data Acquisition System.

Stable three point bend test
Tests were performed at the same temperatures and using the same servohydraulic universal testing machine as that used in the splitting test. At each temperature, three specimens were tested.

The tests were carried out according to the RILEM TC50 standard recommendations ussing a full weight compensation [11]. All the tests were stable, and stability was achieved by running the test in crack mouth opening displacement (CMOD) control. The CMOD rate during the test was 0.03 mm/minute. To measure the CMOD a clip-on gauge MTS 632.03C-51 extensometer of ± 4.0 mm span range was used.

Deflection was measured as the relative displacement of the central loading head relative to the beam supports. Two MTS 63211C-21 extensometers of ± 3.75 mm span range were used for this purpose, placed one at each side of the specimen. During the test, the load, the extensometer output signal and the temperatures of the thermocouples attached to the specimen were continuously recorded until complete failure, via an Automatic Data Acquisition System.

EXPERIMENTAL RESULTS

Results of the splitting tensile test

The main results of the splitting tensile test are summarized in Table 2 which gives the number of tests N, the mean value of the splitting tensile strength f_{st}, the standard deviation S, and the coefficient of variation C_v for each temperature.

TABLE 2

SPLITTING TEST RESULTS

Temperature (ºC)	Test N	f_{st} (MPa)	S (MPa)	C_v (%)
20	3	3.84	0.18	4.8
-20	3	5.30	0.26	4.9
-70	3	6.65	0.79	12.0
-120	3	6.85	0.46	6.7
-170	3	7.11	0.24	3.4

f_{st} splitting tensile strength, S standard deviation and C_v coefficient of variation.

Results of the three point bend test

Table 3 summarizes the main results obtained from the three-point-bend test with the number of tests N, the nominal strength σ_{NR} obtained from equation (1), the energy of fracture G_F , and the elastic modulus E at each temperature. Values in square brackets indicate the standard deviation.

$$\sigma_{NR} = 6P_U/BD \qquad (1)$$

were P_u is the peak load recorded during the test, B the specimen thickness and D the specimen depth.

TABLE 3

THREE POINT BEND TEST RESULTS

Temperature (ºC)	Test N	σ_{NR} (MPa)	G_F (N/m)	E (GPa)
20	3	1.35 [0.01]	80 [5.5]	39.8
-20	3	2.02 [0.07]	175 [11.0]	37.6
-70	3	2.56 [0.09]	240 [11.5]	41.8
-120	3	2.77 [0.19]	271 [27.0]	46.6
-170	3	2.43 [0.08]	279 [17.0]	41.6

The elastic modulus was obtained from the initial compliance of the Load-CMOD curve using the expression for the CMOD given by Tada, Paris and Irwin [8]. The energy of fracture was obtained by the procedure described in the RILEM TC50 draft recommendation with the corrections proposed by the authors [9, 10, 11].

Parameters of the bilinear softening curve.

From the results of both the splitting test and stable three point bend test, the main parameters of the softening function were determined. This function is the relevant material property within the framework of the cohesive crack model used to characterize the fracture behavior of the material. In practice, to determine the softening curve we assumed that it can be appropriately described by a bilinear curve as shown in Figure 1. This hypothesis is usually adopted for quasi brittle materials such as concrete. In the Figure, the key points of the curve are marked with an open symbol. A complete description of the method used to fit the bilinear curve parameters, i.e. “the general bilinear fit method for the softening curve of concrete”, is given in reference [12].

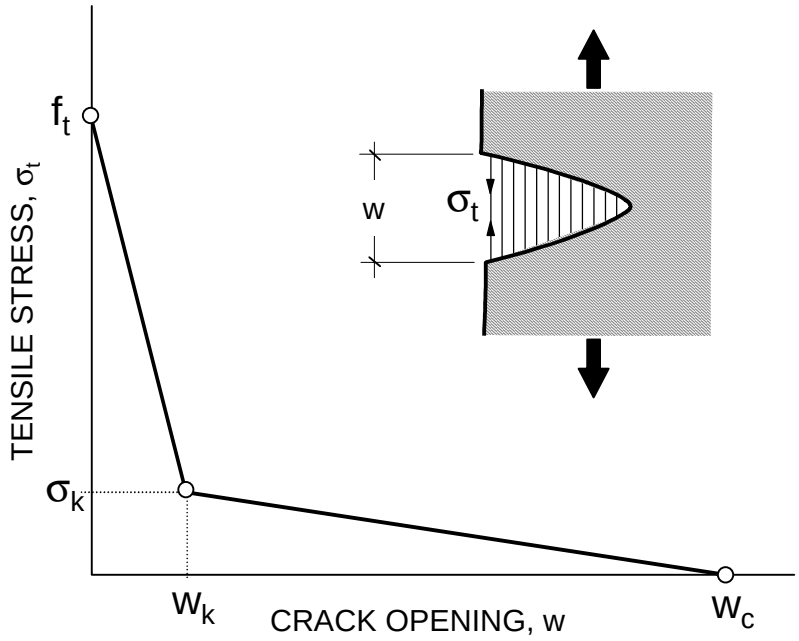

Figure 1: Bilinear softening curve

Table 4 indicates the parameters of the softening curves obtained at each test temperature. It includes the tensile strength f_t, the coordinates, σ_k and w_k, of the curve break-point, and the critical crack opening, w_c. Note that the value of the splitting tensile strength was assumed as a true value of the tensile strength. In a recent in-depth study of the splitting test the authors demonstrated that for the specimen size and width of the bearing strips used in the present tests , this assumption is accurate [13, 14].

In Table 4, the characteristic length, l_{ch} calculated from equation (2) is also included. In the context of the cohesive crack model, l_{ch} is a fracture parameter used to describe the intrinsic brittleness of the material.

$$l_{ch} = EG_F / f_t^2 \quad (2)$$

TABLE 4

PARAMETERS OF THE BILINEAR SOFTENING CURVES

Temperature (ºC)	f_t (MPa)	w_k (μm)	σ_k (MPa)	w_c (μm)	l_{ch} (mm)
20	3.84	19	0.43	201	216
-20	5.30	40	0.48	314	234
-70	6.65	41	0.77	281	226
-120	6.85	47	0.82	337	269
-170	7.11	22	2.00	198	229

DISCUSSION AND FINAL REMARKS

Influence of low temperatures on splitting tensile strength and fracture energy

Figure 2 shows the evolution of the splitting tensile strength with the temperature. The errors bars correspond to ± the standard deviation. The experimental results show that the splitting tensile strength of concrete at low temperature displays a noticeable increment, especially from 20 to –70ºC. Below –70ºC the influence of the temperature on the tensile strength becomes less pronounced and the strength values seem to approach an asymptotic value.

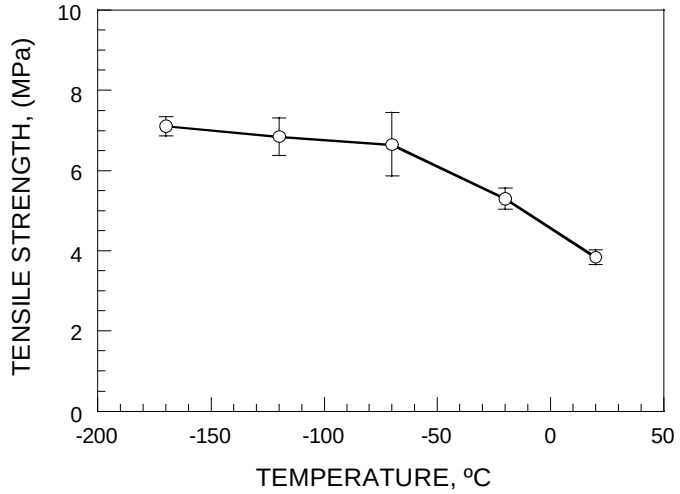

Figure 2: Effect of low temperatures on the splitting tensile strength

Figure 3 shows the evolution of the fracture energy with the temperature. The error bars correspond to ± the standard deviation. As shown in the Figure, the fracture energy of concrete increases as the temperature decreases but seems to approach an asymptote at temperatures below –120°C.

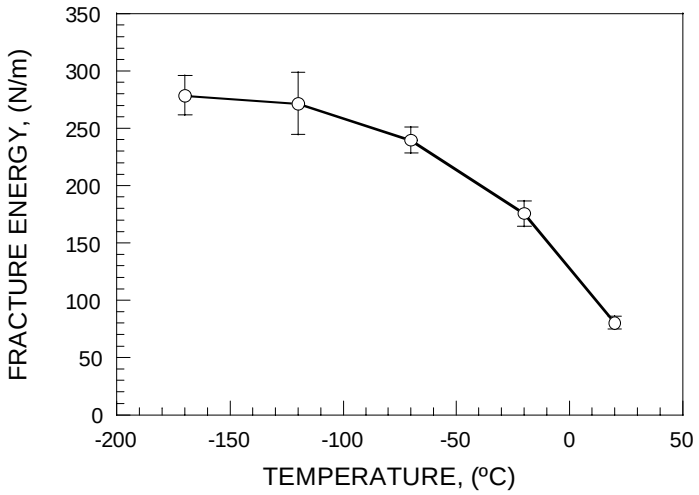

Figure 3: Effect of low temperatures on the fracture energy

The increase of the splitting tensile strength and the fracture energy at low temperatures can be explained by the freezing of water in the bulk of the concrete. During cooling, the free water trapped in the complex network of capillary pores of the hardened cement paste solidify, gradually sealing the pores and strengthening the material. However, this is only a qualitative explanation, and further basic research is needed to understand the complex thermodynamic phenomena taking place during cooling.

Influence of low temperature on the softening curve

Figure 4 shows, for each test temperature, the softening curves of concrete obtained from the results included in Table 4. Note that from 20 to –120 ºC, the softening curves are similar, in that the slopes of the two linear segments are close to each other. Between –120 and –170 ºC the softening curve changes abruptly. At –170°C the initial slope of the curve becomes steeper and the tail of the curve shorter.

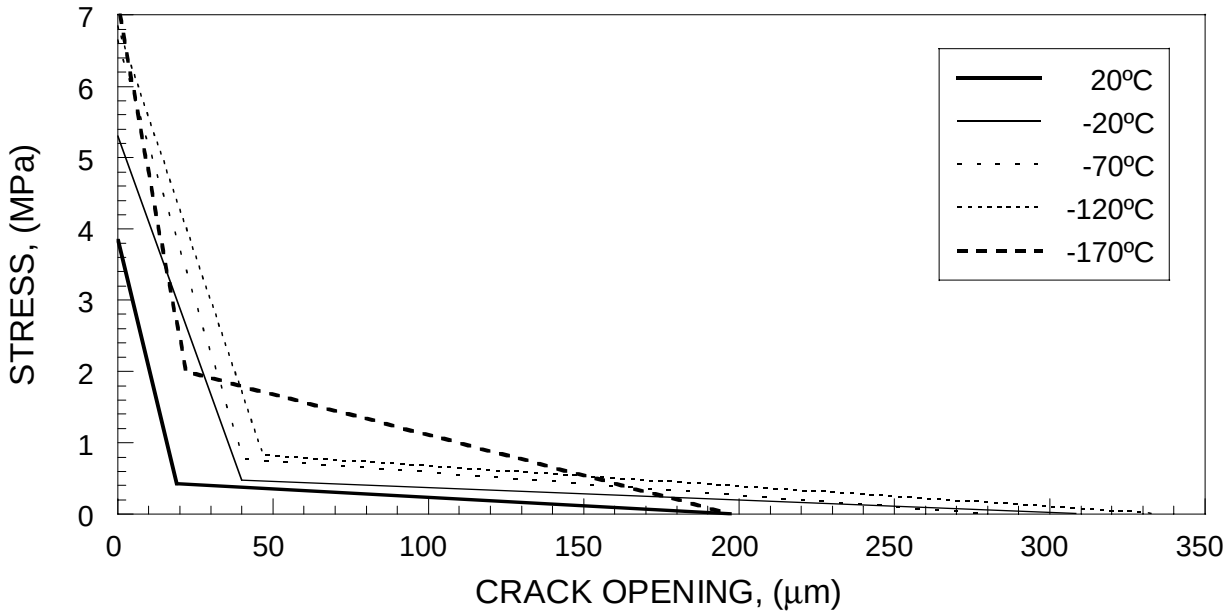

Figure 4: Softening cuve of concrete at different temperatures

The similitudes and differences of the softening curves become more evident when these curves are plotted nondimensionally by dividing the tensile stress by the tensile strength and the crack opening by the fracture energy to tensile strength ratio (G_F/f_t). The dimensionless softening curves obtained in this way are shown in Figure 5. Note that except at –170ºC, the shapes of the curves are very close to each other.

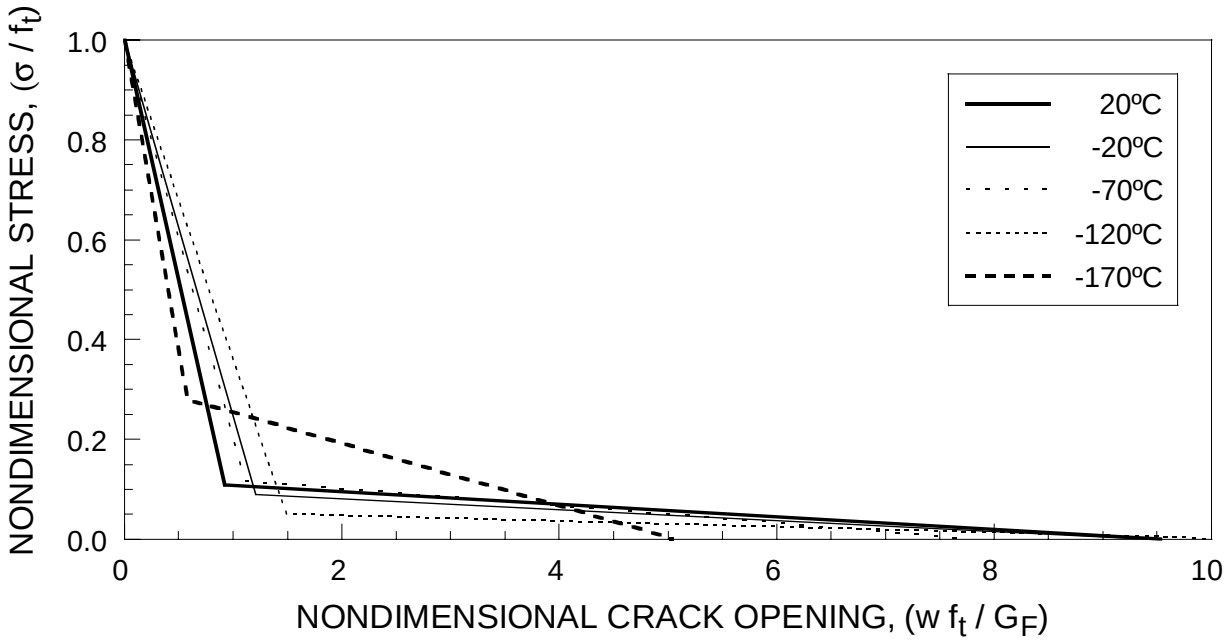

Figure 5: Dimensionless softening cuve of concrete at different temperatures

Finally, Figure 6 shows the evolution of the characteristic length l_{ch} with the temperature. It is worth remembering that if both the shape of the softening curve and the size of the structure are held constant, the brittlenes of the structure may be measured by the inverse of the characteristic length. The results in Figure 6, show that l_{ch} remains approximately constant or increases slightly at low temperatures. This indicates that lowering the temperature does not increase the brittleness of concrete.

The main practical conclusion is that even though the tensile strength, the modulus of elasticity and the energy of fracture, increase strongly at low temperatures, the dimensionless softening curve and the characteristic length remain similar down to –120°C. An abrupt change is observed in the softening curve at –170 ºC, an effect that deserves further research.

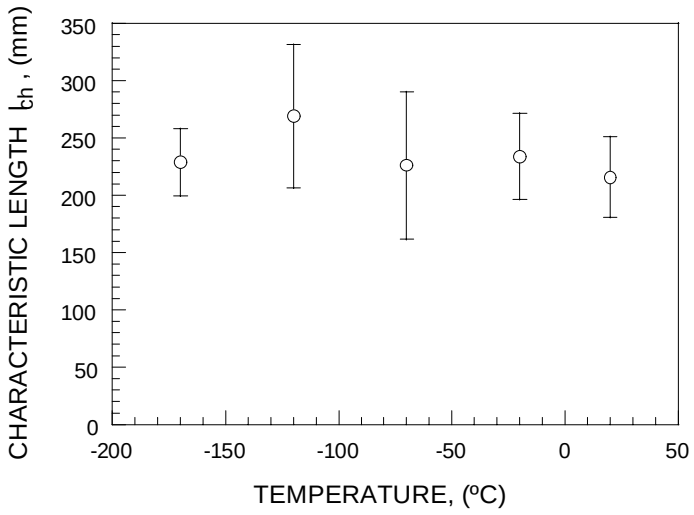

Figure 6: Evolution of the characteristic length with temperature.

REFERENCES

1. Elices, M., Rostasy, F. S., Faas, W. M. and Wiedemann, G. (1982). FIP State of the Art Report.
2. The Concrete Society (1982). *Cryogenic Concrete*. Construction Press.
3. The Concrete Societies of the Netherlands and the U.K. (1983). *Cryogenic Concrete*. Concrete Society.
4. Maturana, P., Planas, J. and Elices, M. (1990). *Engineering Fracture Mechanics* **35**, 827.
5. Elices, M., Planas, J. and Maturana, P. (1987). In: Fracture of Concrete and Rock, pp. 106-116, Shah, S.P. and Swartz, S.E. (Eds), Springer-Verlag, New York.
6. ASTM C496-85 (1986). In: *Annual Book of ASTM Standards* 4 (04.02), pp 337-342.
7. RILEM Draft Recommendation (1985). *Materials and Structures* **18**, 285.
8. Tada, H., Paris, P. and Irwin, G. (1985). *The Stress Analysis of Cracks Handbook*, Del Research Corporation, St Louis, Missouri.
9. Guinea, G.V., Planas, J. and Elices, M., (1992). *Materials and Structures* **25**, 212.
10. Planas, J., Elices, M., and Guinea, G.V. (1992). *Materials and Structures* **25**, 305.
11. Elices, M., Guinea, G.V. and Planas, J. (1992). *Materials and Structures* **25**, 327.
12. Guinea, G.V. Planas, J. and Elices, M. (1994). *Materials and Structures* **27**, 99.
13. Rocco, C., Guinea, G.V., Planas, J. and Elices, M. (1999). *Materials and Structures* **32**, 210.
14. Rocco, C., Guinea, G.V., Planas, J. and Elices, M. (1999). *Materials and Structures* **32**, 437.